

## Heavy-ion potentials derived from strong-absorption-model parametrizations of the scattering function

L. J. Allen,\* H. Fiedelvey, and S. A. Sofianos

*Department of Physics, University of South Africa, P.O. Box 392, Pretoria, 0001, South Africa*

K. Amos and C. Steward

*School of Physics, University of Melbourne, Parkville, Victoria 3052, Australia*

(Received 19 February 1991)

Heavy-ion interaction potentials for 360 MeV  $^{12}\text{C}-^{12}\text{C}$  and 1503 MeV  $^{16}\text{O}-^{40}\text{Ca}$  are derived from solutions of the fixed energy, inverse scattering problem. A semiclassical (WKB) approximation is used to obtain those solutions when various strong-absorption-model parametrized  $S$  functions are defined from fits to the differential cross-section data. The extracted potentials vary significantly in their absorption components within the sensitive radial regions.

### I. INTRODUCTION

In most studies of heavy-ion collisions, the central feature is the optical potential. To define that potential extensive data from the elastic scattering of two heavy ions have to be taken and, usually, analyzed by direct solution of the relevant Schrödinger equation with a parametrized form of the optical potential [1]. Of particular interest are those optical potentials at intermediate energies resulting from folding nuclear density profiles with appropriate two-nucleon  $G$  matrices [2].

The connection between the optical-model potentials and data (differential cross sections primarily) are the scattering functions  $S_l(k)$ . In the direct approach, variations of the optical-potential parameters associated with an assumed potential shape are made from which predictions of elastic cross sections are calculated to compare with data. This results in a set of best-fit parameters for the assumed potential shape. But the connection can be made in the reverse direction by a solution of the inverse scattering problem at fixed energy [3]. In this case no assumptions are made concerning the potential shape. When the  $S$  function is known for all  $l$ , a solution of the inverse problem gives a unique scattering potential. Thus, to use an inversion method necessitates interpolation upon tables of  $S_l(k)$  that "best fit" data; however, those tables may be generated. For intermediate energies many partial waves are involved in data analyses and the associated  $S_l(k)$  follow quite smooth trends. For these reasons, scattering functions defined by older and quite widely applied methods of analysis of heavy-ion scattering, namely, the strong-absorption-model (SAM) approach [4], are especially useful. From the earliest simple prescription [5], a number of parametrized forms of such  $S$  functions have been defined. Of the set, those designated hereafter as the McIntyre [6], Frahn-Venter (FV) [7], and Ericson [8], are of particular interest. All three parametrized forms have been used and their results compared by Mermaz [9] in his study of  $^{12}\text{C}$  and  $^{16}\text{O}$  scattering off a range of targets and at disparate projectile energies. The ambiguities occurring in optical-model-

parameter fits to the data apparently do not show up in the SAM-type fits.

Solutions of the inverse quantal scattering problem at fixed energy are most readily obtained using a semiclassical (WKB) approximation [10,11], when applicable. The WKB approximation produced good results in the case of  $^{12}\text{C}-^{12}\text{C}$  scattering at energies ranging from 360 to 2400 MeV, when the McIntyre parametrized form of  $S$  functions was used [12] (as proved by testing the reproduction of the input  $S$  functions). The potentials obtained also agreed well with the best phenomenological optical-model potentials through the sensitive radial regions.

Herein we consider the effects of using different parametrized forms of  $S$  functions upon the potentials one can extract by using WKB inversion. Two scattering cases are considered specifically. They are  $^{12}\text{C}-^{12}\text{C}$  scattering at 360 MeV and  $^{16}\text{O}-^{40}\text{Ca}$  scattering at 1503 MeV. The differential cross-section data [13,14] have been analyzed with McIntyre, FV, and Ericson model  $S$  functions by Mermaz [9] and comparable fits have been found to the data. The results of our calculations and the conclusion we have drawn are presented in Secs. IV and V, respectively, and follow brief reviews of the SAM  $S$  function parametrizations and of the WKB inversion scheme.

### II. PARAMETRIZATIONS OF SAM $S$ FUNCTIONS

The scattering function for elastic scattering of heavy ions is the central feature of both SAM and WKB inversion model calculations and it is expressed in terms of a phase-shift function as

$$S_l(l) = \exp(2i\delta_l(k)) \\ = |S_l(k)| \exp[2i \operatorname{Re}(\delta_l(k))] . \quad (1)$$

Strong absorption within a scattering process is characterized by

$$|S_l(k)| \ll 1 \quad \text{for } l < l_g , \quad (2)$$

where  $l_g$  is the "grazing" angular-momentum value

which, in turn, relates to the “strong-absorption radius,”  $R_{SA}$ . While this radius has been defined by semiclassical formulas [4] such as

$$kR_{SA} = \eta + [\eta^2 + (l_g + \frac{1}{2})^2]^{1/2}, \quad (3)$$

where  $\eta$  is the Sommerfeld parameter for reduced mass,  $\mu$ , i.e.,  $Z_1 Z_2 e^2 \mu / (\hbar^2 k)$ , it is more common to use a simpler definition [1], namely,

$$R_{SA} = r_a (A_P^{1/3} + A_T^{1/3}) + \Delta, \quad (4)$$

with  $r_a \approx 1.1$  fm and  $\Delta \approx 2.5$  MeV.

The earliest and simplest SAM prescription was defined by Blair [5] as the “sharp cutoff” model since the choice

$$|S_l| = \begin{cases} 0 & \text{if } l < l_g \\ 1 & \text{if } l > l_g \end{cases}, \quad (5)$$

was made. This proved to be a too drastic approximation for nuclear diffraction scattering processes. The nuclear surface plays an important role and a more realistic description has a smooth variation of  $|S_l|$  values (between 0 and 1) over a range of  $l$  values about  $l_g$ . Given that the underlying scattering potential has an exponential tail, the WKB approximation [4] estimates that spread to vary as

$$\Delta \approx R_{SA}^{1/2} k^{3/2} a (kR_{SA} - \eta) / (kR_{SA} - 2\eta)^{1/2}, \quad (6)$$

where  $a$  is the coordinate-space potential diffusivity. There are three model prescriptions that reflect such a more realistic variation and which have been widely used, and we consider each of these here. The first is the smooth parametrization of  $S_l(k)$  proposed by McIntyre *et al.* [6]. Explicitly, the McIntyre parametrization of SAM  $S$  functions is

$$|S_l^{(\text{McIntyre})}(k)| = \{1 + \exp[(l_g - l)/\Delta]\}^{-1} \quad (7)$$

and

$$\text{Re}(\delta_l^{(\text{McIntyre})}(k)) = \mu \{1 + \exp[(l - l'_g)/\Delta']\}^{-1}. \quad (8)$$

This five-parameter model suffices to permit excellent fits to differential cross sections from as diverse elastic-scattering experiments as alpha nucleus through 360 MeV  $^{12}\text{C}$ - $^{12}\text{C}$  to 1503 MeV  $^{16}\text{O}$ - $^{40}\text{Ca}$  reactions. The second of the SAM  $S$  matrix parametrizations is that specified by Venter and Frahn [7] which is defined by

$$\text{Re}(S_l^{(\text{FV})}(k)) = |S_l^{(\text{McIntyre})}|, \quad (9)$$

$$\text{Im}(S_l^{(\text{FV})}(k)) = \frac{\mu}{\Delta} |S_l^{(\text{McIntyre})}| (1 - |S_l^{(\text{McIntyre})}|),$$

wherein  $|S_l^{(\text{McIntyre})}|$  is as defined in Eq. (7). Finally, we consider a parametrization given by Ericson [8], namely,

$$S_l^{(\text{Ericson})}(k) = \{1 + \exp(i\phi) \exp[(l_g - l)/\Delta]\}^{-1}. \quad (10)$$

All three SAM parametrizations were used by Mermaz [9] in his study of 360 and 1016 MeV  $^{12}\text{C}$ - $^{12}\text{C}$  cross sections and of 1503 MeV  $^{16}\text{O}$  ions scattering from  $^{12}\text{C}$ ,  $^{40}\text{Ca}$ ,  $^{90}\text{Zr}$  and  $^{208}\text{Pb}$ . He found that the McIntyre five-parameter prescription gave the best fits to all of the data. The Frahn-Venter and Ericson models worked well when data are reminiscent of a Fresnel diffraction pattern. The fits with either of these latter parametrizations to high-energy data from the light-ion targets were mostly qualitative at best.

In the cases of 360 MeV  $^{12}\text{C}$ - $^{12}\text{C}$  scattering and of 1503 MeV  $^{16}\text{O}$ - $^{40}\text{Ca}$  scattering, the three parametrizations give comparable and good fits to the differential cross-section data. The pertinent values of the parameters as determined by Mermaz [9] are given in Table I for completeness. Included therein are the  $\chi^2$  values (per data point) that, with the possible exception of the FV  $^{12}\text{C}$ - $^{12}\text{C}$  result, reflect the similar qualities of fits to data.

### III. INVERSE SCATTERING AT FIXED ENERGY IN THE WKB APPROXIMATION

Since details of the inverse scattering, fixed energy problem and of the use of the WKB approximation to facilitate evaluation of inversion potentials have been presented in the literature [3,10,11], only the salient features will be given herein. The input data for inversion are the scattering phase shifts (equivalently the empirical scattering,  $S$  functions). In the WKB approximation, phase shifts relate to a quasipotential,  $Q(\sigma)$ , by [11]

$$\delta(\lambda) = -\frac{1}{2E} \int_{\lambda}^{\infty} Q(\sigma) \frac{\sigma}{\sqrt{\sigma^2 - \lambda^2}} d\sigma, \quad (11)$$

where  $\lambda = l + \frac{1}{2}$  and  $E$  is the center-of-mass energy, and that quasipotential is defined in terms of the classical deflection functions

TABLE I. Parameter values of the scattering functions.

	$^{12}\text{C}$ - $^{12}\text{C}$			$^{16}\text{O}$ - $^{40}\text{Ca}$		
	McIntyre	FV	Ericson	McIntyre	FV	Ericson
$l_g$	40.719	40.94	40.876	183.041	176.08	175.43
$\Delta$	6.228	2.67	3.658	20.271	10.14	14.43
$\mu$	3.0445	3.4358	4.4041	14.60		
$l'_g$	30.344		133.873			
$\Delta'$	4.134		17.519			
$\phi$			-1.2641			-1.3492
$\chi^2$	5.4	10.0	4.6	4.3	6.8	6.2

$$\theta(\lambda) = 2d\delta(\lambda)/d\lambda \quad (12)$$

by

$$Q(\sigma) = \frac{2E}{\pi} \int_{\sigma}^{\infty} \frac{\theta(\lambda)}{\sqrt{\lambda^2 - \sigma^2}} d\lambda \\ \equiv \frac{4E}{\pi} \frac{1}{\sigma} \frac{d}{d\sigma} \left[ \int_{\sigma}^{\infty} \frac{\delta(\lambda)\lambda}{\sqrt{\lambda^2 - \sigma^2}} d\lambda \right]. \quad (13)$$

Then, with wave number  $k$ , the inverse potential is related to  $Q(\sigma)$  by

$$V(kr) = E \{ 1 - \exp[-Q(\sigma)/E] \} \quad (14)$$

with

$$r = (\sigma/k) \exp[Q(\sigma)/2E]. \quad (15)$$

The potential so specified is unique provided that there is a one-to-one correspondence between  $r$  and  $\sigma$ .

The key feature in this prescription is the integral of Eq. (13) and the rational representation [1] of  $\delta(\lambda)$ , namely,

$$\delta(\lambda) = \frac{1}{2i} \ln[S(\lambda)] = \frac{1}{2i} \ln \left[ \prod_{n=1}^N \frac{\lambda^2 - \beta_n^2}{\lambda^2 - a_n^2} \right], \quad (16)$$

which makes that integral analytic. Thus, by using empirical  $S$  functions [ $S(\lambda) = S_l(k)$ ] and mapping them with the rational representation, evaluation of the quasi-potential (and thence the inverse scattering potential) is straightforward. But the experimental  $S$  functions in the presence of Coulomb forces are not readily represented in this way. Thus, with the identification

$$S_{\text{exp}} = S_{\text{nucl}} S_{\text{Coul}}, \quad (17)$$

wherein  $S_{\text{nucl}}$  are the nuclear  $S$  functions and  $S_{\text{Coul}}$  are those of point Coulomb scattering, viz.,

$$S_{\text{Coul}}(\lambda) = \Gamma(\lambda + 0.5 + i\eta) / \Gamma(\lambda + 0.5 - i\eta) \quad (18)$$

( $\eta$  is the Coulomb parameter), we seek instead inversion of the modified  $S$  functions of rational form,

$$S_{\text{mod}} = S_{\text{exp}} / S_{\text{back}}, \quad (19)$$

where  $S_{\text{back}}$  is a "background" scattering function of the form [11]

$$S_{\text{back}}(\lambda) = \exp[i\eta \ln(\lambda^2 + \lambda_c^2)] \quad (20)$$

that involves  $\lambda_c$ , a cutoff parameter. The corresponding inversion potential to  $S_{\text{back}}$ ,  $V_{\text{back}}$ , is a quasi-Coulomb potential which asymptotically (large  $r$ ) behaves as the Coulomb potential but is not singular at the origin. In this way we avoid the problems experienced by Kujawski [10] in using a point Coulomb background potential. But, of particular importance, besides giving modified  $S$  functions that can be represented very well in rational form,  $S_{\text{back}}$  itself can be inverted classically to give  $V_{\text{back}}$  to high accuracy.

With the inverted potentials  $V_{\text{mod}}$  and  $V_{\text{back}}$ , we construct

$$V_{\text{exp}} = V_{\text{mod}} + V_{\text{back}} \equiv V_{\text{nucl}} + V_{\text{Coul}}^{\text{FS}}, \quad (21)$$

wherein the Coulomb potential is taken to be that of a charged sphere of radius  $R_c$ , namely,

$$V_{\text{Coul}}^{\text{FS}} = \begin{cases} 2\eta/r & \text{if } r > R_c, \\ \frac{\eta}{R_c} (3 - r^2/R_c^2) & \text{if } r < R_c \end{cases} \quad (22)$$

so that the nuclear potential is given by

$$V_{\text{nucl}}(r) = V_{\text{mod}} + V_{\text{back}} - V_{\text{Coul}}^{\text{FS}}. \quad (23)$$

For heavy ions, the numerical and computational efforts required to implement the SAM fitting and WKB inversion are small compared to those of optical-potential fitting.

#### IV. RESULTS

The two reactions chosen for study are diverse. The  $^{12}\text{C}$ - $^{12}\text{C}$  case is one of relatively low incident energy whereas  $^{16}\text{O}$ - $^{40}\text{Ca}$  is at relatively high energy. The  $^{12}\text{C}$ - $^{12}\text{C}$  data defining  $S$ -function parameters are dominantly from "far-side" scattering whereas the  $^{16}\text{O}$ - $^{40}\text{Ca}$  data so used are dominantly of "near-side" scattering [9]. But both data sets show structure in their distributions and both have been successfully analyzed with all three parametrized SAM  $S$  functions.

The results for 360 MeV  $^{12}\text{C}$  on  $^{12}\text{C}$  targets are presented in Figs. 1 and 2. The real parts, the imaginary parts, and the moduli of the three model parametrizations of that reaction data are shown on the left, middle, and right sections of Fig. 1, respectively; the McIntyre, FV, and Ericson model  $S$  functions being displayed by the continuous, dashed, and dotted curves in turn. Clearly, the FV and Ericson  $S$  functions are very similar with, in fact, the only noticeable difference being the size of the imaginary components for angular momenta around the grazing value. Such a difference is enough, however, to vary the  $\chi^2$  of a fit to measured data by a factor of 2 (see Table I). Mermaz [9] observed that this also implies that the Ericson parametrization has a larger (semiclassical) potential diffusivity and smaller Coulomb rainbow angle.

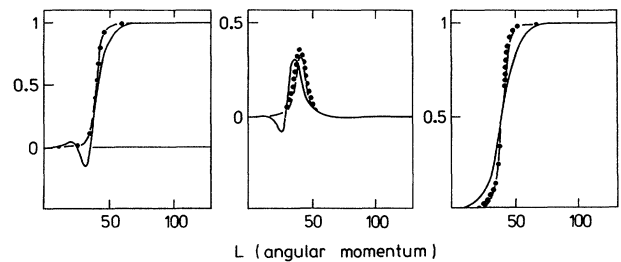


FIG. 1. The  $S$  functions for 360 MeV  $^{12}\text{C}$ - $^{12}\text{C}$  scattering. Displayed are the real parts, imaginary parts, and moduli of SAM parametrizations and in the left, central, and right sections, respectively. The (five-parameter) McIntyre function is shown by the continuous lines while the Frahn-Venter and Ericson functions are given by the dashed and dotted curves, respectively.

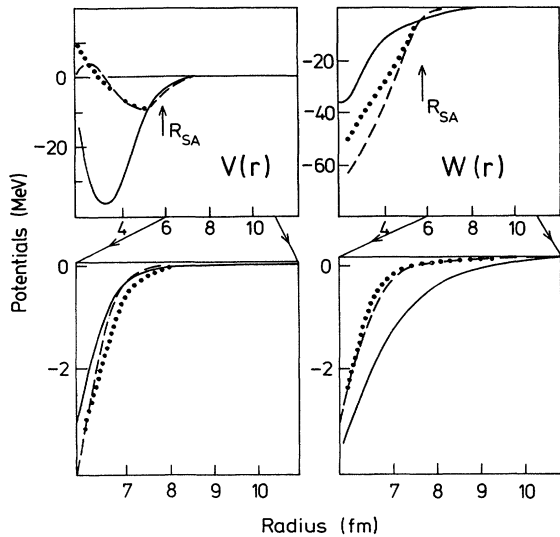


FIG. 2. The 360 MeV  $^{2}\text{C}-^{12}\text{C}$  potentials obtained by WKB inversion of the three parametrized  $S$  functions given in Fig. 1. The real and imaginary components are displayed on the right and left, respectively. The large radius variations are shown on enhanced scale in the bottom segments.

But the McIntyre (five-parameter) data fit gives a much larger diffusivity and nuclear rainbow angle than either of the other two parametrizations, and, as a consequence, gives a smoother, more credible, prediction for larger-angle measured data.

The WKB inverted potentials are shown in Fig. 2 wherein the real and imaginary parts are designated by  $V(r)$  and  $W(r)$ , respectively. These potentials are uniquely determined for each SAM parametrization as long as the WKB inversion method gives single-valued results. This is indeed the case here. The large radius properties of the potentials are enlarged in the bottom sections of this figure. All three potentials,  $V^{(\text{McIntyre})}(r)$ ,  $V^{(\text{FV})}(r)$ , and  $V^{(\text{Ericson})}(r)$  are strongly absorptive within the strong-absorption radius (6.2 fm); so strong, in fact, that the extreme variations in their real and imaginary components within at least 5 fm are of no physical significance. Notch testing of phenomenological optical-model-potential analyses confirm that the sensitive radial region in this case is indeed outside of 5 fm. But within the sensitive radial region the inverted potentials differ with the  $V^{(\text{McIntyre})}(r)$  varying most from the other two. Given the preference [9] for the five-parameter McIntyre fit to data over three-parameter models and despite the similar  $\chi^2$  fit values, these radial variations are significant. Notably, use of  $V^{(\text{McIntyre})}$  in calculations gives minimal oscillatory structure in differential cross-section values at large angles. The inflection in the real part of  $V^{(\text{FV})}(r)$  around 2.75 fm is an indication of an incipient breakdown in the WKB inversion at smaller radii. However, the elastic differential cross section is not sensitive to the potential at these radii.

The results for 1503 MeV  $^{16}\text{O}$  ions elastically scattering off of  $^{40}\text{Ca}$  are displayed in Fig. 3, wherein the various

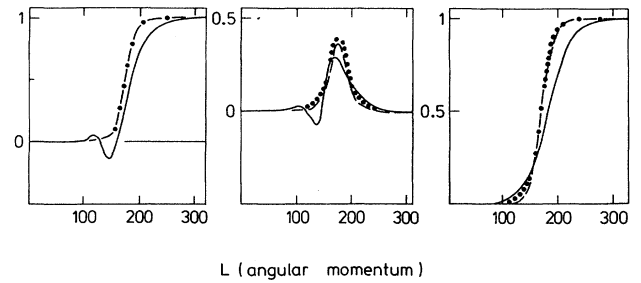


FIG. 3. The SAM parametrized  $S$  functions for 1503 MeV  $^{16}\text{O}-^{40}\text{Ca}$  scattering. Specifications are as given in Fig. 1.

model  $S$  functions are given, and in Fig. 4 wherein the inversion potentials are displayed. Again, the continuous, dashed, and dotted curves are the McIntyre (five-parameter), Frahn-Venter, and Ericson results, respectively. The  $S$ -function variations with  $\lambda$  given in Fig. 3 are similar to those from analysis of the  $^{12}\text{C}-^{12}\text{C}$  scattering. Notably, the five-parameter McIntyre  $S$  function is softer than the others, having a larger effective grazing angular momentum and a larger range of effective contributing partial waves. The associated inversion potentials are shown in Fig. 4. Around the strong-absorption radius (of 7.7 fm), the real parts of these inversion potentials are very similar. The marked difference in  $V^{(\text{McIntyre})}(r)$  from the other two for  $r < 7$  fm is of little significance. But, as with the  $^{12}\text{C}-^{12}\text{C}$  study [12], it is the absorption potential that gives major effects. In the sensitive radial region,  $W^{(\text{McIntyre})}(r)$  is more strongly absorptive and of much larger range than either  $W^{(\text{FV})}(r)$  or  $W^{(\text{Ericson})}(r)$ . Larger-angle scattering data, when measured, should show a preference, we anticipate, for the McIntyre five-parameter form since, as shown by Pato and Hussein [15], the rainbow component of far-side scattering processes dominates above  $6^\circ$  scattering angle in the reaction.

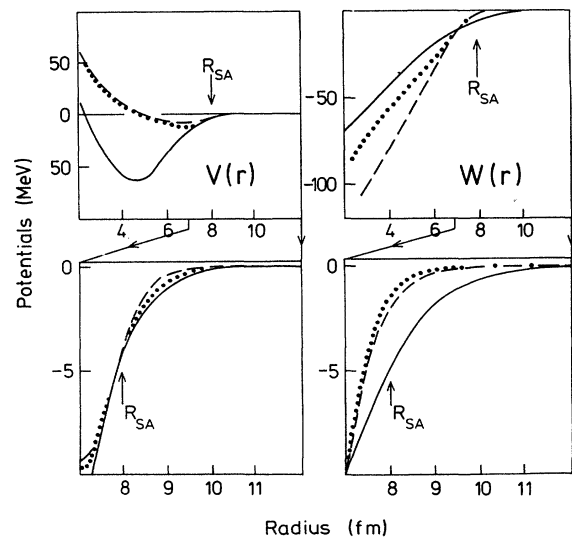


FIG. 4. The WKB inverted potentials for 1503 MeV  $^{16}\text{O}-^{40}\text{Ca}$  scattering. Notation is the same as given in Fig. 2.

## V. CONCLUSIONS

Using a WKB approximation to facilitate the evaluation of inversion potentials, we have compared the  $^{12}\text{C}$ - $^{12}\text{C}$  and  $^{16}\text{O}$ - $^{40}\text{Ca}$  potentials so obtained and from SAM parametrizations of the 360- and 1503-MeV elastic-scattering data of those respective collisions. All three SAM parametrizations considered (McIntyre, Frahn-Venter, and Ericson) give good fits to both sets of data chosen for study. The two data sets result from distinctively different reaction mechanisms as the  $^{12}\text{C}$ - $^{12}\text{C}$  data analyses are dominated by far-side scattering processes whereas the  $^{16}\text{O}$ - $^{40}\text{Ca}$  data analyses are dominated by near-side ones. Nevertheless, the potentials obtained by inversion have similar structure, and, in particular, in the respective sensitive radial regions. Therein, the real parts of the potentials associated with the three separate parametrizations are very similar as is the case for the imaginary parts of the FV and Ericson potentials. The McIntyre parametrization, however, gives a distinctively more absorptive potential in the radial regions about the

strong-absorption radii. But the details of the shapes of these potentials are rather different and, given the equivalent fits to data obtained with the different parametrized  $S$  functions, such a variation is a measure of ambiguities in defining the nuclear part of the heavy-ion potentials based upon the currently available data. Inverse scattering methods highlight the crucial importance of making more extensive and accurate measurements for further understanding of heavy-ion collisions. With such data, the inversion methods will be superior to the direct, parameter-fitting, procedures of data analyses. Besides the simplicity of the inversion scheme, no assumptions are made concerning the potential shape.

Finally, we note the interesting feature, common to all three  $S$ -function inversions, of a short-ranged, repulsive, real potential. The usual parametrized optical-model potentials do not have such form. Some theoretical model potentials do, but usually only for low-energy conditions [16]. However, the current data are not sufficiently sensitive to such short-ranged behavior of the heavy-ion interaction.

---

\*Permanent address: School of Science & Mathematics Education, University of Melbourne, Parkville, Victoria 3052, Australia.

- [1] G. R. Satchler, Nucl. Phys. **A409**, 3c (1983), and references cited therein.
- [2] N. Ohtsuka, M. Shabshiry, R. Linden, H. Mütther, and A. Faessler, Nucl. Phys. **A490**, 715 (1988).
- [3] K. Chadan and P. C. Sabatier, *Inverse Problems in Quantum Scattering Theory* (Springer, Berlin, 1988).
- [4] W. E. Frahn, in *Treatise on Heavy Ion Science*, edited by D. A. Bromley (Plenum, New York, 1984), Vol. 1, p. 135.
- [5] J. S. Blair, Phys. Rev. **95**, 1218 (1954).
- [6] J. A. McIntyre, K. H. Wang, and L. C. Becker, Phys. Rev. **117**, 1337 (1960).
- [7] R. H. Venter and W. E. Frahn, Ann. Phys. (N.Y.) **24**, 243 (1963).
- [8] T. E. O. Ericson, in *Preludes in Theoretical Physics*, edited by A. de Shalit, H. Feshbach, and L. van Hove (North-Holland, Amsterdam, 1966), p. 321.
- [9] M. C. Mermaz, Z. Phys. **A 321**, 613 (1985).
- [10] R. Lipperheide, H. Fiedeldey, and H. Leeb, in *Advanced Methods in the Analysis of Nuclear Scattering Data*, Vol. 236 of *Lecture Notes in Physics*, edited by H. J. Krappe and R. Lipperheide (Springer, Berlin, 1985); E. Kujawski, Phys. Rev. C **8**, 100 (1973).
- [11] H. Fiedeldey, R. Lipperheide, K. Naidoo, and S. A. Sofianos, Phys. Rev. C **30**, 434 (1984).
- [12] L. J. Allen, K. Amos, C. Steward, and H. Fiedeldey, Phys. Rev. C **41**, 2021 (1990).
- [13] M. Buenerd, A. Loomis, J. Chauvin, D. Lebrun, P. Martin, G. Duhamel, J. C. Gordan, and P. de Saintignon, Nucl. Phys. **A424**, 313 (1984).
- [14] P. Roussel-Chomaz, N. Alamanos, F. Auger, J. Barrette, B. Berthier, B. Fernandez, L. Papineau, H. Doubre, and W. Mittig, Nucl. Phys. **A477**, 345 (1988).
- [15] M. P. Pato and M. S. Hussein, Phys. Rep. **189**, 127 (1990).
- [16] D. T. Khoa, A. Faessler, and N. Ohtsuka, J. Phys. G **16**, 1253 (1990).